Environmental responses, not species interactions, determine species synchrony in natural plant communities

Andrew T. Tredennick[1], Claire de Mazancourt[2], Michel Loreau[2], and Peter B. Adler[1]

[1]*Department of Wildland Resources and the Ecology Center, 5230 Old Main Hill, Utah State University, Logan, Utah 84322 USA*

[2]*Centre for Biodiversity Theory and Modelling, Theoretical and Experimental Ecology Station, CNRS and Paul Sabatier University, Moulis, 09200, France*

Keywords: synchrony, compensatory dynamics, environmental stochasticity, demographic stochasticity, interspecific competition, stability

Authorship: ATT, CdM, and PBA designed the research. CdM and ML designed and analyzed the theoretical model. ATT and PBA performed the empirical analysis. All authors contributed to the interpretation and presentation of results. ATT wrote the first draft of the manuscript, and all authors contributed to manuscript revisions.

Running Title: Drivers of species synchrony in natural plant communities

Article Type: Letter

Number of Words: Abstract = 136; Main Text = 4992

Number of References: 46

Number of Tables and Figures: 2 Tables; 3 Figures

Corresponding Author:
Andrew Tredennick
Department of Wildland Resources and the Ecology Center
Utah State University
5230 Old Main Hill
Logan, Utah 84322 USA
Phone: +1-970-443-1599
Fax: +1-435-797-3796
Email: atredenn@gmail.com

Abstract

Temporal asynchrony among species helps diversity to stabilize ecosystem functioning, but identifying the mechanisms that determine synchrony remains a challenge. Here, we refine and test theory showing that synchrony depends on three factors: species responses to environmental variation, interspecific interactions, and demographic stochasticity. We then conduct simulation experiments with empirical population models to quantify the relative importance of these factors in five plant communities. We found that the average synchrony of per capita growth rates, which can range from 0 (perfect asynchrony) to 1 (perfect synchrony), was higher when environmental variation was present (0.62) rather than absent (0.43). Removing interspecific interactions and demographic stochasticity had small effects on synchrony. In these plant communities, where species interactions and demographic stochasticity have little influence, synchrony reflects the covariance in species responses to the environment.

INTRODUCTION

Ecosystems are being transformed by species extinctions (Cardinale et al. 2012), changes in community composition (Vellend et al. 2013, Dornelas et al. 2014), and anthropogenic environmental change (Vitousek et al. 1997), impacting the provisioning and stability of ecosystem services (Loreau et al. 2001, Hooper et al. 2005, Rockstrom et al. 2009). Experiments have provided compelling evidence that decreases in species richness will decrease productivity (Tilman et al. 2001) and the temporal stability of productivity (Tilman et al. 2006, Hector et al. 2010). The stabilizing effect of species richness stems from individual species responding in different ways to environmental fluctuations (environmental stochasticity), or fluctuating asynchronously because of random chance events (demographic stochasticity) (Isbell et al. 2009, Hector et al. 2010, de Mazancourt et al. 2013). Species richness affects synchrony because larger species pools are more likely to contain species that respond disimilarly to environmental conditions (Yachi and Loreau 1999), implying that species losses will reduce ecosystem stability. Even without species losses, abiotic homogenization can weaken compensatory dynamics and, in turn, decrease temporal stability of ecosystem functioning (Hautier et al. 2014). The link between synchrony and stability means that a mechanistic understanding of synchrony can help us predict the impacts of global change on ecosystem stability.

Theory identifies three main determinants of species synchrony: environmental stochasticity, demographic stochasticity, and interspecific interactions (Loreau and de Mazancourt 2008, 2013, Gonzalez and Loreau 2009). For example, in a community composed of large populations (no demographic stochasticity) with weak interspecific interations, community-wide species synchrony should be determined by the covariance of species' responses to the environment (Loreau and de Mazancourt 2008). However, this prediction relies on a relatively simple population model and only holds under two assumptions: (i) species' responses to the environment are similar in magnitude and (ii) all species have similar growth rates. Whether

such theoretical predictions hold in natural communities where species differences are unlikely to be symmetrical is unkown because few studies have explicitly tested theory on the drivers of species synchrony in natural communities (Mutshinda et al. 2009, Thibaut et al. 2012), and they did not consider demographic stochasiticity.

In grasslands, most empirical studies have focused on whether species synchrony is primarily an outcome of species-specific responses to environmental conditions (Hautier et al. 2014) or competition (Gross et al. 2014). Even beyond grassland studies, whether competition or environmental responses drive compensatory dynamics remains controversial (reviewed in Gonzalez and Loreau 2009). In part, controversy remains because quantifying the relative strengths of each driver on the degree of synchrony from the covariance matrix of species abundances (e.g., Houlahan et al. 2007) is impossible. This is because an unbiased null expectation for synchrony does not exist (Loreau and de Mazancourt 2008) and observed synchrony can arise from non-unique combinations of factors (Ranta et al. 2008). For example, weak synchrony of population abundances could reflect positive environmental correlations (synchronizing effect) offset by strong competition (desynchronizing effect), or negative environmental correlations and weak competition.

The best way to quantify the effects of environmental stochasticity, demographic stochasticity, and interspecific interactions is to remove them one-by-one, and in combination. In principle, this could be done in an extremely controlled laboratory setting, but empirically-based models of interacting populations, fit with data sets from natural communities, offer a practical alternative. For example, Mutshinda et al. (2009) fit a dynamic population model to several community time series of insect and bird abundances. They used a statistical technique to decompose temporal variation into competition and environmental components, and found that positively correlated environmental responses among species determined community dynamics. Thibaut et al. (2012) used a similar approach for reef fish and came to a similar conclusion: environmental responses determine synchrony. While a major step forward, Mutshinda et al.'s (2009) and Thibaut et al.'s (2012) modeling technique relied on

abundance data that may or may not reliably capture competitive interactions that occur at the individual level. Furthermore, although both studies quantified the relative importance of environmental stochasticity and interspecific interactions to explain the observed variation of species synchrony, they did not use the model to quantify how much synchrony would change when each factor is removed.

Here, we use multi-species population models fit to long-term demographic data from five semi-arid plant communities to test theory on the drivers of species synchrony. Our objectives are to (1) derive and test theoretical predictions of species synchrony and (2) determine the relative influence of environmental stochasticity, demographic stochasticity, and interspecific interactions on species synchrony in natural plant communities. To achieve these objectives, we first refine theory that has been used to predict the effects of species richness on ecosystem stability (de Mazancourt et al. 2013) and species synchrony (Loreau and de Mazancourt 2008) to generate predictions of community-wide species synchrony under two limiting cases derived from the dynamics of individual species in monoculture. We then confront our theoretical predictions with simulations from the empirically-based population models. Second, we use the multi-species population models to perform simulation experiments that isolate the effects of environmental stochasticity, demographic stochasticity, and interspecific interactions on community-wide species synchrony. Given that our population models capture the essential features of community dynamics important to synchrony (density-dependence, and demographic and environmental stochasticity), and that these models successfully reproduce observed community dynamics (Chu and Adler 2015), perturbing the models can reveal the processes that determine species synchrony in our focal grassland communities.

THEORETICAL MODEL

The model

While existing theory has identified the factors driving synchrony, we do not have a simple expression to predict synchrony in a particular community with all factors operating simultaneously. However, we can derive analytical predictions for species synchrony under special limiting cases. The limiting case predictions we derive serve as baselines to help us interpret results from empirically-based simulations (described below). We focus on synchrony of per capita growth rates, rather than abundances, because growth rates represent the instantaneous response of species to the environment and competition, and are less susceptible to the legacy effects of drift and disturbance (Loreau and de Mazancourt 2008). We present equivalent results for synchrony of species abundances in the Online Supporting Information, and show that they lead to the same overall conclusions as synchrony of per capita growth rates. Following Loreau and de Mazancourt (2008) and de Mazancourt et al. (2013), we define population growth, ignoring observation error, as

$$r_i(t) = \ln N_i(t+1) - \ln N_i(t) \tag{1}$$

$$= r_{mi}\left[1 - \frac{N_i(t) + \sum_{j \neq i} \alpha_{ij} N_j(t)}{K_i} + \sigma_{ei} u_{ei}(t) + \frac{\sigma_{di} u_{di}(t)}{\sqrt{N_i(t)}}\right] \tag{2}$$

where $N_i(t)$ is the biomass of species i in year t, and $r_i(t)$ is its population growth rate in year t. r_{mi} is species i's intrinsic rate of increase, K_i is its carrying capacity, and α_{ij} is the interspecific competition coefficient representing the effect of species j on species i. Environmental stochasticity is incorporated as $\sigma_{ei} u_{ei}(t)$, where σ_{ei}^2 is the environmental variance and u_{ei} are normal random variables with zero mean and unit variance that are independent through time but may be correlated between species. Demographic stochasticity arises from variations in births and deaths among individuals (e.g., same states, different

fates), and is included in the model as a first-order, normal approximation (Lande et al. 2003, de Mazancourt et al. 2013). σ_{di}^2 is the demographic variance and $u_{di}(t)$ are independent normal variables with zero mean and unit variance. To derive analytical predictions we solved a first-order approximation of Equation 2 (de Mazancourt et al. 2013 and Online Supporting Information). Due to the linear approximation approach, our analytical predictions will likely fail in communities where species exhibit large fluctuations due to limit cycles and chaos (Loreau and de Mazancourt 2008). Indeed, one of the advantages of focusing on growth rates rather than abundances is that growth rates are more likely to be well-regulated around an equilibrium value, if the long-term average of a species' growth rate is relatively small (e.g., $r < 2$).

Predictions

Our first prediction assumes no interspecific interactions, no environmental stochasticity, identical intrinsic growth rates, and that demographic stochasticity is operating but all species have identical demographic variances. This limiting case, $\mathcal{M}_D$, represents a community where dynamics are driven by demographic stochasticity alone. Our prediction for the synchrony of per capita growth rates for $\mathcal{M}_D$, $\phi_{R,\mathcal{M}_D}$, is

$$\phi_{R,\mathcal{M}_D} = \frac{\sum_i p_i^{-1}}{\left(\sum_i p_i^{-1/2}\right)^2}, \tag{3}$$

where p_i is the average frequency of species i, $p_i = N_i/N_T$. When all species have identical abundances and $p_i = 1/S$, where S is species richness, synchrony equal 1/S (Loreau and de Mazancourt 2008).

Our second limiting case assumes only environmental stochasticity is operating ($\mathcal{M}_E$). Thus, we assume there are no interspecific interactions, demographic stochasticity is absent, intrinsic growth rates are identical, and environmental variance is identical for all species.

Our prediction for the synchrony of per capita growth rates for $\mathcal{M}_E$, $\phi_{R,\mathcal{M}_E}$, is

$$\phi_{R,\mathcal{M}_E} = \frac{\sum_{i,j} \mathrm{cov}(u_{ei}, u_{ej})}{S^2}, \tag{4}$$

where $\mathrm{cov}(u_{ei}, u_{ej})$ is the standardized covariance of environmental responses between species i and species j. Confronting our theoretical predictions with data requires estimates of species dynamics of large populations (no demographic stochasticity) growing in isolation (no interspecific interactions) to calculate the covariance of species' environmental responses. To estimate environmental responses in natural communities, we turn to our population models built using long-term demographic data.

EMPIRICAL ANALYSIS

Materials and methods

Data We use long-term demographic data from five semiarid grasslands in the western United States (described in detail by Chu and Adler 2015). Each site includes a set of 1-m^2 permanent quadrats within which all individual plants were identified and mapped annually using a pantograph (Hill 1920). The resulting mapped polygons represent basal cover for grasses and canopy cover for shrubs. Data come from the Sonoran desert in Arizona (Anderson et al. 2012), sagebrush steppe in Idaho (Zachmann et al. 2010), southern mixed prairie in Kansas (Adler et al. 2007), northern mixed prairie in Montana (Anderson et al. 2011), and Chihuahuan desert in New Mexico (Anderson et al. in preparation, Chu and Adler 2015) (Table 1).

Calculating observed synchrony The data consist of records for individual plant size in quadrats for each year. To obtain estimates of percent cover for each focal species in each year, we summed the individual-level data within quadrats and then averaged percent cover,

by species, over all quadrats. We calculated per capita growth rates as $\log(x_t) - \log(x_{t-1})$, where x is species' percent cover in year t. Using the community time series of per capita growth rates or percent cover, we calculated community synchrony using the metric of Loreau and de Mazancourt (2008) in the 'synchrony' package (Gouhier and Guichard 2014) in R (R Core Team 2013). Specifically, we calculated synchrony as

$$\phi_r = \frac{\sigma_T^2}{(\sum_i \sigma_{r_i})^2} \tag{5}$$

where σ_{r_i} is the temporal variance of species i's per capita population growth rate (r_i) and σ_T^2 is the temporal variance of the aggregate community-level growth rate. ϕ ranges from 0 at perfect asynchrony to 1 at perfect synchrony (Loreau and de Mazancourt 2008). We use the same equation to calculate observed synchrony of species' percent cover, which we present to relate our results to previous findings, even though we focus on synchrony of growth rates in our model simulations (see below).

Fitting statistical models Vital rate regressions are the building blocks of our dynamic models: an integral projection model (IPM) and an individual-based model (IBM). We followed the approach of Chu and Adler (2015) to fit statistical models for survival, growth, and recruitment (see Online Supporting Information for full details). We modeled survival probability of each genet as function of genet size, temporal variation among years, permanent spatial variation among groups of quadrats, and local neighborhood crowding from conspecific and heterospecific genets. Regression coefficients for the effect of crowding by each species can be considered a matrix of interaction coefficients whose diagonals represent intraspecific interactions and whose off-diagonals represent interspecific interactions (Adler et al. 2010). These interaction coefficients can take positive (facilitative) or negative (competitive) values. We modeled growth as the change in size of a genet from one year to the next, which depends on the same factors as the survival model. We fit the survival and growth regressions using

INLA (Rue et al. 2014), a statistical package for fitting generalized linear mixed effects models via approximate Bayesian inference (Rue et al. 2009), in R (R Core Team 2013). Crowding was treated as a fixed effect without a temporal component because most 95% credible intervals for random year effects on crowding broadly overlapped zero and, in a test case, including yearly crowding effects did not change our results. Spatial (quadrat groupings) variation was treated as a random effect on the intercept and temporal (interannual) variation was treated as random effects on the intercept and the effect of genet size in the previous year (Online Supporting Information).

We modeled recruitment at the quadrat scale, rather than the individual scale, because the original data do not attribute new genets to specific parents (Chu and Adler 2015). Our recruitment model assumes that the number of recruits produced in each year follows a negative binomial distribution with the mean dependent on the cover of the parent species, permanent spatial variation among groups, temporal variation among years, and inter- and intraspecific interactions as a function of total species' cover in the quadrat. We fit the recruitment model using a hierarchical Bayesian approach implemented in JAGS (Plummer 2003) using the 'rjags' package (Plummer 2014) in R (R Core Team 2013). Again, temporal and spatial variation were treated as random effects.

Building dynamic multi-species models Once we have fit the vital rate statistical models, building the population models is straightforward. For the IBM, we initialize the model by randomly assigning plants spatial coordinates, sizes, and species identities until each species achieves a density representative of that observed in the data. We then project the model forward by using the survival regression to determine whether a genet lives or dies, the growth regression to calculate changes in genet size, and the recruitment regression to add new individuals that are distributed randomly in space. Crowding is directly calculated at each time step since each genet is spatially referenced (as in the observed data). Environmental stochasticity is not an inherent feature of IBMs, but is easily included since we fit year-specific

temporal random effects for each vital rate regression. To include temporal environmental variation, at each time step we randomly choose a set of estimated survival, growth, and recruitment parameters specific to one observation year. For all simulations, we ignore the spatial random effect associated with variation among quadrat groups, so our simulations represent an average quadrat for each site.

The IPM uses the same vital rate regressions as the IBM (Rees and Ellner 2009, Rees et al. 2014), but it is spatially implicit and does not include demographic stochasticity. Following Chu and Adler (2015), we use a mean field approximation that captures the essential features of spatial patterning to define the crowding index at each time step (Supporting Online Information). Temporal variation is included in exactly the same way as for the IBM. For full details on the IPMs we use, see Chu and Adler (2015).

Simulation experiments We performed simulation experiments where drivers (environmental stochasticity, demographic stochasticity, or interspecific interactions) were removed one-by-one and in combination. To remove interspecific interactions, we set the off-diagonals of the interaction matrix for each vital rate regression to zero. This retains intraspecific interactions, and thus density-dependence, and results in simulations where species are growing in isolation. We cannot definitively rule out the effects of species interactions on all parameters, meaning that a true monoculture could behave differently than our simulations of a population growing without interspecific competitors. To remove the effect of a fluctuating environment, we removed the temporal (interannual) random effects from the regression equations. To remove the effect of demographic stochasticity, we use the IPM rather than the IBM because the IPM does not include demographic stochasticity (demographic stochasticity cannot be removed from the IBM). Since the effect of demographic stochasticity on population dynamics depends on population size (Lande et al. 2003), we can control the strength of demographic stochasticity by simulating the IBM on areas (e.g. plots) of different size. Indeed, results from an IBM with infinite population size would converge on results from the IPM.

Given computational constraints, the largest landscape we simulate is a 25 m^2 plot.

We conducted the following six simulation experiments: (1) IBM: All drivers (environmental stochasticity, demographic stochasticity, or interspecific interactions) present; (2) IPM: Demographic stochasticity removed; (3) IBM: Environmental stochasticity removed; (4) IBM: Interspecific interactions removed; (5) IPM: Interspecific interactions and demographic stochasticity removed; (6) IBM: Interspecific interactions and environmental stochasticity removed. We ran IPM simulations for 2,000 time steps, after an initial 500 iteration burn-in period. This allowed species time to reach their stable size distribution. We then calculated the synchrony of species' per capita growth rates over 100 randomly selected contiguous 50 time-step sections. We ran IBM simulations for 100 time steps, and repeated the simulations 100 times for each simulation experiment. From those, we retained only the simulations in which no species went extinct due to demographic stochasticity. Synchrony was calculated over the 100 time steps for each no extinction run within a model experiment. To explore the effect of demographic stochasticity in different sized populations, we ran simulations (1) and (6) on plot sizes of 1, 4, 9, 16, and 25 m^2. All other IBM simulations were run on a 25 m^2 landscape.

Results from our simulation experiments also allow us to test our theoretical predictions. First, in the absence of interspecific interactions and demographic stochasticity, populations can only fluctuate in response to the environment. Therefore, we can use results from simulation (5) to estimate the covariance of species' responses to the environment ($\mathrm{cov}(u_{ie}, u_{je})$) and parameterize Equation 4. Parameterizing Equation 3 does not require simulation output because the only parameters are the species' relative abundances. Second, simulations (5) and (6) represent the simulated version of our limiting case theoretical predictions. Thus, we directly test the theoretical predictions by comparing them to observed synchrony and simulated synchrony.

Results

Synchrony of species' per capita growth rates at our study sites range from 0.36 to 0.89 and synchrony of percent cover ranged from 0.15 to 0.92 (Table 2). Synchrony tends to be higher in communities with few species (Arizona and New Mexico) and/or with relatively high temporal variability in percent cover (e.g., Montana). Synchrony is lowest in Idaho, the only data set that includes two life forms: a shrub and three perennial grasses (Table 1). Synchrony of per capita growth rates and CV of percent cover are positively correlated (Pearson's $\rho = 0.72$). For all five communities, species synchrony from IPM and IBM simulations closely approximated observed synchrony (Fig. S1). IBM-simulated synchrony is consistently, but only slightly, lower than IPM-simulated synchrony (Fig. S1), likely due to the desynchronizing effect of demographic stochasticity.

Across the five communities, our limiting case predictions closely matched synchrony from the corresponding simulation experiment (Fig. 1 and Table S1). The correlation between our analytical predictions and simulated synchrony was 0.97 for $\phi_{R,\mathcal{M}_D}$ and 0.997 for $\phi_{R,\mathcal{M}_E}$. The largest difference between predicted and simulated synchrony was 0.05 in New Mexico for $\phi_{R,\mathcal{M}_D}$ (Table S1).

Simulation experiments revealed that removing environmental fluctuations has the largest impact on synchrony, leading to a reduction in synchrony of species growth rates in four out of five communities (Fig. 1). Removing environmental fluctuations ("No E.S" simulations) decreased synchrony by 33% in Arizona, 48% in Kansas, 39% in Montana, and 40% in New Mexico. Only in Idaho did removing environmental fluctuations cause an increase in synchrony (Fig. 1), but the effect was small (9% increase; Table S2). Overall, species' temporal random effects in the statistical vital rate models are positively correlated (Table S3). Species interactions are weak in these communities (Table S4 and Chu and Adler 2015), and removing interspecific interactions had little effect on synchrony (Fig. 1; "No Comp." simulations). Removing interspecific interactions caused, at most, a 5% change in synchrony

(Fig. 1). Removing demographic stochasticity ("No D.S." simulations) caused synchrony to increase slightly in all communities (Fig. 1), with an average 6% increase over synchrony from IBM simulations on a $25m^2$ area.

The desynchronizing effect of demographic stochasticity, which increases as population size decreases, modestly counteracted the synchronizing force of the environment, but not enough to lower synchrony to the level observed when only demographic stochasticity is operating (Fig. 2). In the largest, 25 m^2 plots, synchrony was driven by environmental stochasticity (e.g., $\mathcal{M}_E$). At 1 m^2, synchrony reflected demographic stochasticity and environmental stochasticity (e.g., between $\mathcal{M}_E$ and $\mathcal{M}_D$). For context, population sizes increased from an average of 17 individuals per community in 1 m^2 IBM simulations to an average of 357 individuals per community in 25 m^2 IBM simulations.

For all five communities, the synchrony of species' growth rates when growing in isolation almost perfectly matched species synchrony in polyculture (Fig. 3). Results for synchrony of percent cover are qualitatively similar, but simulation results were more variable and less consistent with analytical predictions and observed synchrony (Online Supporting Information, Figs. S2-S3).

DISCUSSION

Our study produced four main findings that were generally consistent across five natural plant communities: (1) limiting-case predictions from the theoretical model were well-supported by simulations from the empirical models; (2) demographic stochasticity decreased community synchrony, as expected by theory, and its effect was largest in small populations; (3) environmental fluctuations increased community synchrony relative to simulations in constant environments because species-specific responses to the environment were positively, though not perfectly, correlated; and (4) interspecific interactions were weak and therefore had little impact on community synchrony. We also found that analyses based on synchrony

of species' percent cover, rather than growth rates, were uninformative (Figs. S2-S3) since the linear approximation required for analytical predictions is a stronger assumption for abundance than growth rates, especially given relatively short time-series (Online Supporting Information). Thus, our results provide further evidence that it is difficult to decipher mechanisms of species synchrony from abundance time series, as expected by theory (Loreau and de Mazancourt 2008). Observed synchrony of per capita growth rates was positively correlated with the variability of percent cover across our focal communities, which confirms that we are investigating an important process underlying ecosystem stability.

Simulations support theoretical predictions

Our theoretical predictions were derived from a simple model of population dynamics and required several simplifying assumptions, raising questions about their relevance to natural communities. For example, the species in our communities do not have equivalent environmental and demographic variances (Figs. S4-S7), as required by our predictions. However, the theoretical predictions closely matched results from simulations of population models fit to long-term data from natural plant communities (Table 3). Such strong agreement between our analytical predictions and the simulation results should inspire confidence in the ability of simple models to inform our understanding of species synchrony even in complex natural communities, and allows us to place our simulation results within the context of contemporary theory.

Demographic stochasticity decreases synchrony

Demographic stochasticity partially counteracted the synchronizing effects of environmental fluctuations and interspecific interactions on per capita growth rates, but only when populations were small (Fig. 2), in agreement with theory (Loreau and de Mazancourt 2008). Even in small populations, however, demographic stochasticity was not strong enough to

compensate the synchronizing effects of environmental fluctuations and match the analytical prediction where only demographic stochasticity is operating ($\mathcal{M}_D$ in Fig. 2). These results confirm the theoretical argument by Loreau and de Mazancourt (2008) that independent fluctuations among interacting species in a non-constant environment should be rare. Only in the Idaho community does synchrony of per capita growth rates approach $\mathcal{M}_D$ in a non-constant environment (Fig. 2). This is most likely due to the strong effect of demographic stochasticity on the shrub *Artemisia tripartita* since even a 25 m^2 quadrat would only contain a few individuals of that species.

Our analysis of how demographic stochasticity affects synchrony demonstrates that synchrony depends on the observation area. As the observation area increases, population size increases and the desynchronizing effect of demographic stochasticity lessens (Fig. 2). Thus, our results suggest that community-wide species synchrony will increase as the observation area increases, rising from $\mathcal{M}_D$ to $\mathcal{M}_E$. Such a conclusion assumes, however, that species richness remains constant as observation area increases, which is unlikely (Taylor 1961). Recent theoretical work has begun to explore the linkage between ecosystem stability and spatial scale (Wang and Loreau 2014, 2016), and our results suggest that including demographic stochasticity in theoretical models of metacommunity dynamics may be important for understanding the role of species synchrony in determining ecosystem stability across spatial scales.

Environmental fluctuations drive community synchrony

In large populations where interspecific interactions are weak, synchrony is expected to be driven exclusively by environmental fluctuations (Equation 4). Under such conditions community synchrony should approximately equal the synchrony of species' responses to the environment (Loreau and de Mazancourt 2008). Two lines of evidence lead us to conclude that environmental fluctuations drive species synchrony in our focal plant communities. First,

in our simulation experiments, removing interspecific interactions resulted in no discernible change in community-wide species synchrony of per capita growth rates (Fig. 1). Second, removing environmental fluctuations from simulations consistently reduced synchrony (Fig. 1), and the synchrony of species in isolation was a very strong predictor of synchrony of species in polyculture (Fig. 3). Our results lead us to conclude that environmental fluctuations, not species interactions, are the primary driver of community-wide species synchrony in the communities we studied. Given accumulating evidence that niche differences in natural communities are large (reviewed in Chu and Adler 2015), and thus species interactions are likely to be weak, our results may be general in natural plant communities.

In the Idaho community, removing environmental fluctuations did not cause a large decrease in synchrony. However, that result appears to be an artifact. Removing environmental variation results in a negative invasion growth rate for *A. tripartita*. Although we only analyzed IBM runs in which *A. tripartita* had not yet gone extinct, it was at much lower abundance than in the other simulation runs. When we removed *A. tripartita* from all simulations, the Idaho results conformed with results from all other sites: removing environmental stochasticity caused a significant reduction in species synchrony (Fig. S8). Our main results for Idaho (Fig. 2), with *A. tripartita* included, demonstrate how the processes that determine species synchrony interact in complex ways. *A. tripartita* has a facilitative effect on each grass species across all vital rates, except for a small competitive effect on *H. comata*'s survival probability (Tables S8-S10). At the same time, all the perennial grasses have negative effects on each other for each vital rate (Tables S8-S10). We know synchrony is affected by interspecific competition (Loreau and de Mazancourt 2008), but how facilitative effects manifest themselves is unknown. The interaction of facilitation and competition is clearly capable of having a large effect on species synchrony, and future theoretical efforts should aim to include a wider range of species interactions.

A challenge to the generality of our results is that we were only able to model common, co-occuring species (see Chu and Adler 2015). Most communities are dominated by few common

407 species and many rare species (McGill et al. 2007), meaning that the low number of common
408 species in our focal commiunities is not unusual. Rather, the generality of our results hinges
409 upon the influence of rare species. Rare species could be kept at low densities by competitive
410 suppression due to strong interspecific interactions. If we had been able to model rare species,
411 we might have found a larger effect of competition on community synchrony. However,
412 recent theory predicts that persistent rare species may actually experience even weaker
413 interspecific competition, and thus stronger niche differences, than common species (Yenni et
414 al. 2012), in which case synchrony would remain predominantly driven by environmental
415 responses. Rare species could also be limited by generalist natural enemies whose effects
416 are density-independent but alter competitive hierarchies (Mordecai 2011). Under such
417 conditions, synchrony will depend on the degree of pathogen-induced fitness differences and
418 the pathogen's response to environmental conditions. Neither our model nor current theory
419 explicitly considers the effects of pathogens on species synchrony, and this highlights the
420 need for theoretical work on the interaction between mechanisms of species coexistence and
421 mechanisms of species synchrony (Loreau 2010).

422 **Interspecific interactions had little impact on community synchrony**

423 We expected community synchrony of per capita growth rates to decrease when we removed
424 interspecific interactions (Loreau and de Mazancourt 2008). We found that community
425 synchrony was virtually indistinguishable between simulations with and without interspecific
426 interactions (Fig. 2). The lack of an effect of interspecific interactions on synchrony is in
427 contrast to a large body of theoretical work that predicts a strong role for competition in
428 creating compensatory dynamics (Tilman 1988) and a recent empirical analysis (Gross et al.
429 2014).

430 Our results do not contradict the idea that competition can lead to compensatory
431 dynamics, but they do highlight the fact that interspecific competition must be relatively

strong to influence species synchrony. The communities we analyzed are composed of species with very little niche overlap (Chu and Adler 2015) and weak interspecific interactions (Tables S1, S3-S17). Mechanistic consumer-resource models (Lehman and Tilman 2000) and phenomenological Lotka-Volterra models (Lehman and Tilman 2000, Loreau and de Mazancourt 2013) both confirm that the effect of competition on species synchrony diminishes as niche overlap decreases. In that sense, our results are not surprising: interspecific interactions are weak, so of course removing them does not affect synchrony.

However, our results do contrast with a recent analysis of several biodiversity-ecosystem functioning experiments showing that competition drives species synchrony in grasslands (Gross et al. 2014). The apparent inconsistency between our results and those of Gross et al. (2014) may be explained by the differences between our studies. Gross et al.'s results are based on rapidly assembling experimental communities that are, at most, 11 years old. The natural, relatively undisturbed communities we studied consist of species that have co-occurred for decades (Chu and Adler 2015) and represent a much later stage of community assembly. In theory, species interactions should weaken through time as community assembly proceeds (Kokkoris et al. 1999), meaning that in biodiversity-ecosystem functioning experiments the processes driving competitive exclusion are still operating. Such communities may be highly influenced by transient, but strong, interspecific competition that can mask the synchronizing effects of the environment. In contrast, synchrony may be driven by environmental fluctuations in older communities. In other words, the dominant driver of community synchrony should shift from competition to environmental fluctuations through time. One way to test this prediction is to continue collecting data from biodiversity-ecoystem functioning experiments and conduct the analysis of Gross et al. (2014) every few years.

Our conclusion that species interactions have little impact on synchrony only applies to single trophic level communities. Species interactions almost certainly play a strong role in multi-trophic communities where factors such as resource overlap (Vasseur and Fox 2007), dispersal (Gouhier et al. 2010), and the strength of top-down control (Bauer et al. 2014) are

all likely to affect community synchrony.

CONCLUSIONS

Species-specific responses to temporally fluctuating environmental conditions is an important mechanism underlying asynchronous population dynamics and, in turn, ecosystem stability (Loreau and de Mazancourt 2013). When we removed environmental variation, we found that synchrony decreased in four out of the five grassland communities we studied (Fig. 2). A tempting conclusion is that our study confirms that compensatory dynamics are rare in natural communities, and that ecologically-similar species will exhibit synchronous dynamics (e.g., Houlahan et al. 2007). Such a conclusion misses an important subtlety. The perennial grasses we studied do have similar responses to the environment (Table S2), which will tend to synchronize dynamics. However, if community-wide species synchrony is less than 1, as it is in all our focal communities, some degree of compensatory dynamics must be present (Loreau and de Mazancourt 2008). In agreement with other studies (Rocha et al. 2011, Vasseur et al. 2014), we find that environmental responses are primarily responsible for the degree of synchrony among ecologically-similar species. This result contrasts with a recent analysis of several biodiversity-ecosystem functioning experiments showing that competition drives community synchrony (Gross et al. 2014). Recently assembled communities, such as experimental plots, may exhibit strong species interactions that will weaken over time (Kokkoris et al. 1999). Future research on the influence of community assembly on synchrony could reconcile inconsistent observations on the biotic and abiotic forces that jointly drive community dynamics.

ACKNOWLEDGMENTS

This work was funded by the National Science Foundation through a Postdoctoral Research Fellowship in Biology to ATT (DBI-1400370) and a CAREER award to PBA (DEB-1054040).

CdM and ML were supported by the TULIP Laboratory of Excellence (ANR-10-LABX-41). We thank the original mappers of the permanent quadrats at each site and the digitizers in the Adler lab, without whom this work would not have been possible. Compute, storage, and other resources from the Division of Research Computing in the Office of Research and Graduate Studies at Utah State University are gratefully acknowledged. We also thank three anonymous reviewers who provided critical feedback that improved the manuscript.

References

Adler, P. B., S. P. Ellner, and J. M. Levine. 2010. Coexistence of perennial plants: An embarrassment of niches. Ecology Letters 13:1019–1029.

Adler, P. B., W. R. Tyburczy, and W. K. Lauenroth. 2007. Long-term mapped quadrats from Kansas prairie: demographic information for herbaceous plants. Ecology 88:2673.

Anderson, J., M. P. McClaran, and P. B. Adler. 2012. Cover and density of semi-desert grassland plants in permanent quadrats mapped from 1915 to 1947. Ecology 93:1492–1492.

Anderson, J., L. Vermeire, and P. B. Adler. 2011. Fourteen years of mapped, permanent quadrats in a northern mixed prairie, USA. Ecology 92:1703.

Bauer, B., M. Vos, T. Klauschies, and U. Gaedke. 2014. Diversity, Functional Similarity, and Top-Down Control Drive Synchronization and the Reliability of Ecosystem Function. The American Naturalist 183:394–409.

Cardinale, B. J., J. E. Duffy, A. Gonzalez, D. U. Hooper, C. Perrings, P. Venail, A. Narwani, G. M. Mace, D. Tilman, D. A. Wardle, A. P. Kinzig, G. C. Daily, M. Loreau, and J. B. Grace. 2012. Biodiversity loss and its impact on humanity. Nature 489:59–67.

Chu, C., and P. B. Adler. 2015. Large niche differences emerge at the recruitment stage to stabilize grassland coexistence. Ecological Monographs 85:373–392.

de Mazancourt, C., F. Isbell, A. Larocque, F. Berendse, E. De Luca, J. B. Grace, B. Haegeman,

H. Wayne Polley, C. Roscher, B. Schmid, D. Tilman, J. van Ruijven, A. Weigelt, B. J. Wilsey, and M. Loreau. 2013. Predicting ecosystem stability from community composition and biodiversity. Ecology Letters 16:617–625.

Dornelas, M., N. J. Gotelli, B. McGill, H. Shimadzu, F. Moyes, C. Sievers, and A. E. Magurran. 2014. Assemblage time series reveal biodiversity change but not systematic loss. Science 344:296–9.

Gonzalez, A., and M. Loreau. 2009. The Causes and Consequences of Compensatory Dynamics in Ecological Communities. Annual Review of Ecology, Evolution, and Systematics 40:393–414.

Gouhier, T. C., and F. Guichard. 2014. Synchrony: quantifying variability in space and time. Methods in Ecology and Evolution 5:524–533.

Gouhier, T. C., F. Guichard, and A. Gonzalez. 2010. Synchrony and Stability of Food Webs in Metacommunities. The American Naturalist 175:E16–E34.

Gross, K., B. J. Cardinale, J. W. Fox, A. Gonzalez, M. Loreau, H. W. Polley, P. B. Reich, and J. van Ruijven. 2014. Species richness and the temporal stability of biomass production: a new analysis of recent biodiversity experiments. The American naturalist 183:1–12.

Hautier, Y., E. W. Seabloom, E. T. Borer, P. B. Adler, W. S. Harpole, H. Hillebrand, E. M. Lind, A. S. MacDougall, C. J. Stevens, J. D. Bakker, Y. M. Buckley, C. Chu, S. L. Collins, P. Daleo, E. I. Damschen, K. F. Davies, P. a Fay, J. Firn, D. S. Gruner, V. L. Jin, J. a Klein, J. M. H. Knops, K. J. La Pierre, W. Li, R. L. McCulley, B. a Melbourne, J. L. Moore, L. R. O'Halloran, S. M. Prober, A. C. Risch, M. Sankaran, M. Schuetz, and A. Hector. 2014. Eutrophication weakens stabilizing effects of diversity in natural grasslands. Nature 508:521–5.

Hector, A., Y. Hautier, P. Saner, L.Wacker, R. Bagchi, J. Joshi, M. Scherer-Lorenzen, E. M. Spehn, E. Bazeley-White, M.Weilenmann, M. C. Caldeira, P. G. Dimitrakopoulos, J. a. Finn, K. Huss-Danell, A. Jumpponen, and M. Loreau. 2010. General stabilizing effects of plant

533 diversity on grassland productivity through population asynchrony and overyielding. Ecology
534 91:2213–2220.

535 Hooper, D., F. Chapin III, and J. Ewel. 2005. Effects of biodiversity on ecosystem functioning:
536 a consensus of current knowledge. Ecological Monographs 75:3–35.

537 Houlahan, J. E., D. J. Currie, K. Cottenie, G. S. Cumming, S. K. M. Ernest, C. S. Findlay,
538 S. D. Fuhlendorf, U. Gaedke, P. Legendre, J. J. Magnuson, B. H. McArdle, E. H. Muldavin,
539 D. Noble, R. Russell, R. D. Stevens, T. J. Willis, I. P. Woiwod, and S. M. Wondzell. 2007.
540 Compensatory dynamics are rare in natural ecological communities. Proceedings of the
541 National Academy of Sciences of the United States of America 104:3273–3277.

542 Isbell, F. I., H. W. Polley, and B. J. Wilsey. 2009. Biodiversity, productivity and the temporal
543 stability of productivity: Patterns and processes. Ecology Letters 12:443–451.

544 Kokkoris, G. D., A. Y. Troumbis, and J. H. Lawton. 1999. Patterns of species interaction
545 strength in assembled theoretical competition communities. Ecology Letters 2:70–74.

546 Lande, R., S. Engen, and B.-E. Saether. 2003. Stochastic population dynamics in ecology
547 and conservation.

548 Lehman, C. L., and D. Tilman. 2000. Biodiversity, Stability, and Productivity in Competitive
549 Communities. The American Naturalist 156:534–552.

550 Loreau, M. 2010. From Populations to Ecosystems: Theoretical Fondations for a New
551 Ecological Synthesis.

552 Loreau, M., and C. de Mazancourt. 2008. Species synchrony and its drivers: neutral and
553 nonneutral community dynamics in fluctuating environments. The American Naturalist
554 172:E48–E66.

555 Loreau, M., and C. de Mazancourt. 2013. Biodiversity and ecosystem stability: A synthesis
556 of underlying mechanisms. Ecology Letters 16:106–115.

557 Loreau, M., S. Naeem, P. Inchausti, J. Bengtsson, J. P. Grime, A. Hector, D. U. Hooper, M.

A. Huston, D. Raffaelli, B. Schmid, D. Tilman, and D. A. Wardle. 2001. Biodiversity and ecosystem functioning: current knowledge and future challenges. Science 294:804–808.

McGill, B. J., R. S. Etienne, J. S. Gray, D. Alonso, M. J. Anderson, H. K. Benecha, M. Dornelas, B. J. Enquist, J. L. Green, F. He, A. H. Hurlbert, A. E. Magurran, P. A. Marquet, B. A. Maurer, A. Ostling, C. U. Soykan, K. I. Ugland, and E. P. White. 2007. Species abundance distributions: Moving beyond single prediction theories to integration within an ecological framework. Ecology Letters 10:995–1015.

Mordecai, E. A. 2011. Pathogen impacts on plant communities: Unifying theory, concepts, and empirical work. Ecological Monographs 81:429–441.

Mutshinda, C. M., R. B. O'Hara, and I. P. Woiwod. 2009. What drives community dynamics? Proceedings of the Royal Society B: Biological Sciences 276:2923–2929.

Plummer, M. 2003. JAGS: A Program for Analysis of Bayesian Graphical Models Using Gibbs Sampling. Pages 20–22 *in* Proceedings of the 3rd international workshop on distributed statistical computing (dSC 2003). march.

Plummer, M. 2014. rjags: Bayesian graphical models using MCMC.

R Core Team. 2013. R: A language and environment for statistical computing.

Ranta, E., V. Kaitala, M. S. Fowler, J. Laakso, L. Ruokolainen, and R. O'Hara. 2008. Detecting compensatory dynamics in competitive communities under environmental forcing. Oikos 117:1907–1911.

Rees, M., and S. P. Ellner. 2009. Integral projection models for populations in temporally varying environments. Ecological Monographs 79:575–594.

Rees, M., D. Z. Childs, and S. P. Ellner. 2014. Building integral projection models: A user's guide.

Rocha, M. R., U. Gaedke, and D. a. Vasseur. 2011. Functionally similar species have similar dynamics. Journal of Ecology 99:1453–1459.

583 Rockstrom, J., J. Rockstrom, W. Steffen, W. Steffen, K. Noone, K. Noone, A. Persson, A.
584 Persson, F. S. Chapin, F. S. Chapin, E. F. Lambin, E. F. Lambin, T. M. Lenton, T. M.
585 Lenton, M. Scheffer, M. Scheffer, C. Folke, C. Folke, H. J. Schellnhuber, H. J. Schellnhuber,
586 B. Nykvist, B. Nykvist, C. A. de Wit, C. A. de Wit, T. Hughes, T. Hughes, S. van der Leeuw,
587 S. van der Leeuw, H. Rodhe, H. Rodhe, S. Sorlin, S. Sorlin, P. K. Snyder, P. K. Snyder, R.
588 Costanza, R. Costanza, U. Svedin, U. Svedin, M. Falkenmark, M. Falkenmark, L. Karlberg,
589 L. Karlberg, R. W. Corell, R. W. Corell, V. J. Fabry, V. J. Fabry, J. Hansen, J. Hansen, B.
590 Walker, B. Walker, D. Liverman, D. Liverman, K. Richardson, K. Richardson, P. Crutzen, P.
591 Crutzen, J. A. Foley, and J. A. Foley. 2009. A safe operating space for humanity. Nature
592 461:472–475.

593 Rue, H., S. Martino, and N. Chopin. 2009. Approximate Bayesian Inference for Latent
594 Gaussian Models Using Integrated Nested Laplace Approximations. Journal of the Royal
595 Statistical Society, Series B 71:319–392.

596 Rue, H., S. Martino, F. Lindgren, D. Simpson, A. Riebler, and E. Teixeira. 2014. INLA:
597 Functions which allow to perform full Bayesian analysis of latent Gaussian models using
598 Integrated Nested Laplace Approximaxion.

599 Taylor, L. R. 1961. Aggregation, Variance and the Mean. Nature 189:732–735.

600 Thibaut, L. M., S. R. Connolly, and H. P. A. Sweatman. 2012. Diversity and stability of
601 herbivorous fishes on coral reefs. Ecology 93:891–901.

602 Tilman, D. 1988. Plant strategies and the dynamics and structure of plant communities.
603 Plant strategies and the dynamics and structure of plant communities.:360 pp.

604 Tilman, D., P. B. Reich, and J. M. H. Knops. 2006. Biodiversity and ecosystem stability in a
605 decade-long grassland experiment. Nature 441:629–632.

606 Tilman, D., P. B. Reich, J. Knops, D. Wedin, T. Mielke, and C. Lehman. 2001. Diversity
607 and productivity in a long-term grassland experiment. Science 294:843–845.

608 Vasseur, D. a, J. W. Fox, A. Gonzalez, R. Adrian, B. E. Beisner, M. R. Helmus, C. Johnson,
609 P. Kratina, C. Kremer, C. de Mazancourt, E. Miller, W. a Nelson, M. Paterson, J. a Rusak,
610 J. B. Shurin, and C. F. Steiner. 2014. Synchronous dynamics of zooplankton competitors
611 prevail in temperate lake ecosystems. Proceedings. Biological sciences / The Royal Society
612 281:20140633.

613 Vasseur, D. A., and J. W. Fox. 2007. Environmental fluctuations can stabilize food web
614 dynamics by increasing synchrony. Ecology Letters 10:1066–1074.

615 Vellend, M., L. Baeten, I. H. Myers-Smith, S. C. Elmendorf, R. Beauséjour, C. D. Brown, P.
616 De Frenne, K. Verheyen, and S. Wipf. 2013. Global meta-analysis reveals no net change in
617 local-scale plant biodiversity over time. Proceedings of the National Academy of Sciences of
618 the United States of America 110:19456–9.

619 Vitousek, P. M., H. a Mooney, J. Lubchenco, and J. M. Melillo. 1997. Human Domination of
620 Earth' s Ecosystems. Science 277:494–499.

621 Wang, S., and M. Loreau. 2014. Ecosystem stability in space: α, β and γ variability. Ecology
622 Letters 17:891–901.

623 Wang, S., and M. Loreau. 2016. Biodiversity and ecosystem stability across scales in
624 metacommunities. Ecology Letters.

625 Yachi, S., and M. Loreau. 1999. Biodiversity and ecosystem productivity in a fluctuating
626 environment: the insurance hypothesis. Proceedings of the National Academy of Sciences of
627 the United States of America 96:1463–1468.

628 Yenni, G., P. B. Adler, and S. K. Morgan Ernest. 2012. Strong self-limitation promotes the
629 persistence of rare species. Ecology 93:456–461.

630 Zachmann, L., C. Moffet, and P. Adler. 2010. Mapped quadrats in sagebrush steppe: long-
631 term data for analyzing demographic rates and plant–plant interactions. Ecology 91:3427.

Tables

Table 1: Site descriptions and focal species.

Site Name	Biome	Location (Lat, Lon)	Obs. Years	Species
New Mexico	Chihuahuan Desert	32.62° N, 106.67° W	1915-1950	*Bouteloua eriopoda* *Sporobolus flexuosus*
Arizona	Sonoran Desert	31°50' N, 110°53' W	1915-1933	*Bouteloua eriopoda* *Bouteloua rothrockii*
Kansas	Southern mixed prairie	38.8° N, 99.3° W	1932-1972	*Bouteloua curtipendula* *Bouteloua hirsuta* *Schizachyrium scoparium*
Montana	Northern mixed prairie	46°19' N, 105°48' W	1926-1957	*Bouteloua gracilis* *Hesperostipa comata* *Pascopyrum smithii* *Poa secunda*
Idaho	Sagebrush steppe	44.2° N, 112.1° W	1926-1957	*Artemisia tripartita* *Pseudoroegneria spicata* *Hesperostipa comata* *Poa secunda*

Table 2: Observed synchrony among species' per capita growth rates (ϕ_R), observed synchrony among species' percent cover (ϕ_C), the coefficient of variation of total community cover, and species richness for each community. Species richness values reflect the number of species analyzed from the community, not the actual richness.

Site	ϕ_R	ϕ_C	CV of Total Cover	Species richness
New Mexico	0.86	0.92	0.51	2
Arizona	0.89	0.80	0.47	2
Kansas	0.54	0.15	0.30	3
Montana	0.53	0.54	0.52	4
Idaho	0.36	0.18	0.19	4

Figures

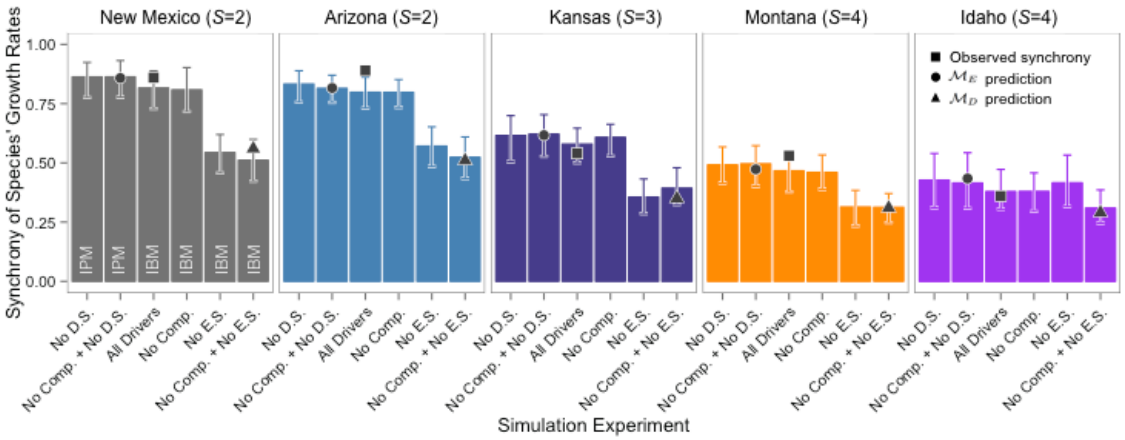

Figure 1: Community-wide species synchrony of per capita growth rates from model simulation experiments. Synchrony of species' growth rates for each study area are from simulation experiments with demographic stochasticity, environmental stochasticity, and interspecific interactions present ("All Drivers"), demographic stochasticity removed ("No D.S."), environmental stochasticity removed ("No E.S."), interspecific interactions removed ("No Comp."), interspecific interactions and demographic stochasticity removed ("No Comp. + No D.S."), and interspecific interactions and environmental stochasticity removed ("No Comp. + No E.S."). Abbreviations within the bars for the New Mexico site indicate whether the IBM or IPM was used for a particular simulation. Error bars represent the 2.5% and 97.5% quantiles from model simulations. All IBM simulations shown in this figure were run on a 25 m^2 virtual landscape. Points show observed and predicted synchrony aligned with the model simulation that corresponds with each observation or analytical predicion.

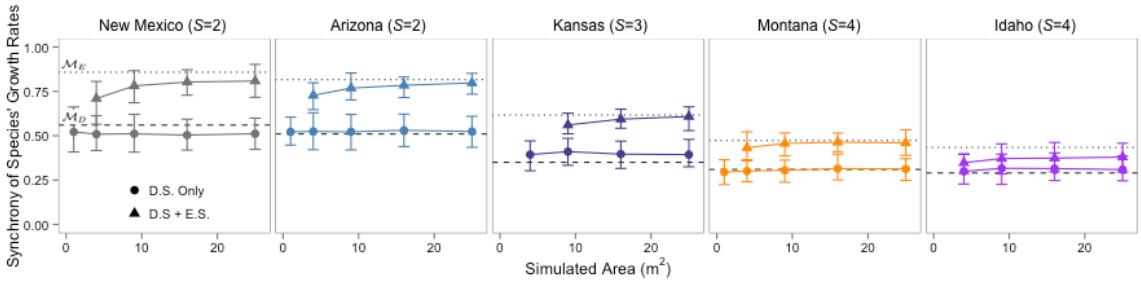

Figure 2: Synchrony of species' growth rates for each study area from IBM simulations across different landscape sizes when only demographic stochastcity is present ("D.S. Only") and when environmental stochasticity is also present removed ("D.S. + E.S."). The horizontal lines show the analytical predictions $\mathcal{M}_D$ (dashed line) and $\mathcal{M}_E$ (dotted line). The strength of demographic stochasticity decreases as landscape size increases because population sizes also increase. Theoretically, "D.S. Only" simulations should remain constant across landscape size, whereas "D.S. + E.S." simulations should shift from the $\mathcal{M}_D$ prediction to the $\mathcal{M}_E$ prediction as landscape size, and thus population size, increases, but only if demographic stochasticity it strong enough to counteract environmental forcing. Error bars represent the 2.5% and 97.5% quantiles from model simulations.

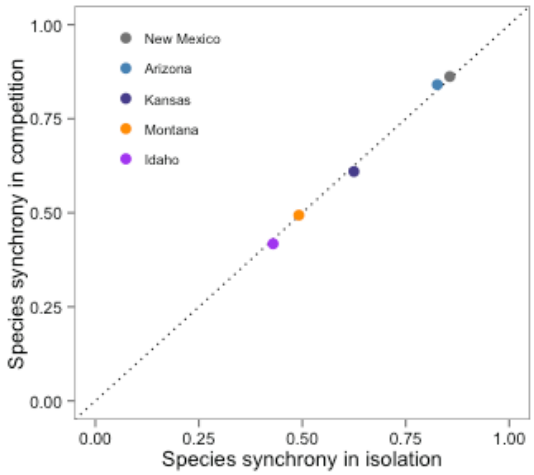

Figure 3: Synchrony of species per capita growth rates when species are growing in isolation (IPM without species interactions) versus synchrony in polycultures (IPM with species interactions). We used the same sequence of random year effects for both simulations (with and without species interactions) to mimic biodiversity-ecosystem functioning experiments. The dashed line is the line of equality. Simulation results in this figure are analagous to "No Comp. + No D.S." (species in isolation) and "No D.S." (species in competition) in Fig. 1, but here we control the time series of random year effects.